The Central Molecular Zone with Mopra

Michael G. Burton and Paul A. Jones

School of Physics, University of New South Wales
Sydney, NSW 2052, Australia

Abstract. We outline a project to map the molecular line emission from the Central Molecular Zone across the 3–12 mm wavebands using the Mopra telescope in Australia. The dataset facilitates use of the CMZ as a template against which observations of molecular emission in other galactic nuclei may be interpreted.

Keywords. Galaxy: center — ISM: molecules

1. Introduction

The Central Molecular Zone (CMZ) contains the greatest collection of molecular gas ($\sim 3 \times 10^7 \, \mathrm{M_\odot}$) within our Galaxy, distributed within its central $\sim 450 \times 150 \, \mathrm{pc}$. It is denser, warmer and more turbulent than the environment within GMCs. Organic species are also widespread throughout the CMZ, and not just confined to compact cores.

With the UNSW–MOPS (an 8 GHz wideband spectrometer), sensitive receivers for the 3, 7 and 12 mm wavebands, on-the-fly mapping and remote operability, the CSIRO 22 m Mopra telescope is capable of undertaking panoramic imaging of the emission from multiple molecular lines of the CMZ with both good spatial (30–$120''$) and high spectral (0.1–2 km/s) resolution. For the Mopra CMZ project† Sgr B2 has been imaged across the entire 3 and 7 mm bands (Jones *et al.* 2008, Jones *et al.* 2011). The CMZ itself has been imaged from 85–93 GHz (Jones *et al.* 2012) and 20–28 GHz (Walsh *et al.* 2011), as well as 42–50 GHz (Jones *et al.* in prep.) and the CO J=1–0 lines from 109–115 GHz (Burton *et al.* in prep.). We summarize here some key results from the 85–93 GHz work.

2. Molecular Imaging

18 molecular lines were bright enough to be imaged across the $2.5° \times 0.6°$ region surveyed. We show peak brightness maps of three of the dense gas tracers in Fig. 1: HCN, HCO^+ and N_2H^+. All maps show the same general structure: a few bright cores on top of widespread emission. PCA analysis highlights locations where secondary structure is evident, for instance variations in the distribution of organic or shocked species.

Wide line profiles are evident across the region, with complex dynamical structures, in places extending over $100 \, \mathrm{km \, s^{-1}}$. The kinematics of the $\sim 10^7 \, \mathrm{M_\odot}$ rotating, twisted cold dust ring extending from Sgr B2 to Sgr C, and identified by Molinari *et al.* (2011) from Herschel data, can be traced in the velocity of the peak emission from the N_2H^+ molecule (see Fig. 2). This molecule traces the location of dense, cold gas.
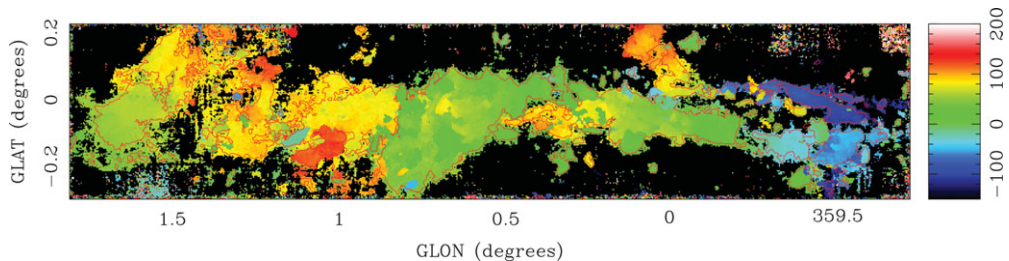
3. Analysis

The isotopologues $H^{13}CN$, $H^{13}CO^+$ and $HN^{13}C$ allow optical depth corrections, facilitating an excitation analysis. To provide a yardstick against which extra-galactic

† See www.phys.unsw.edu.au/mopracmz for full details on the lines observed.
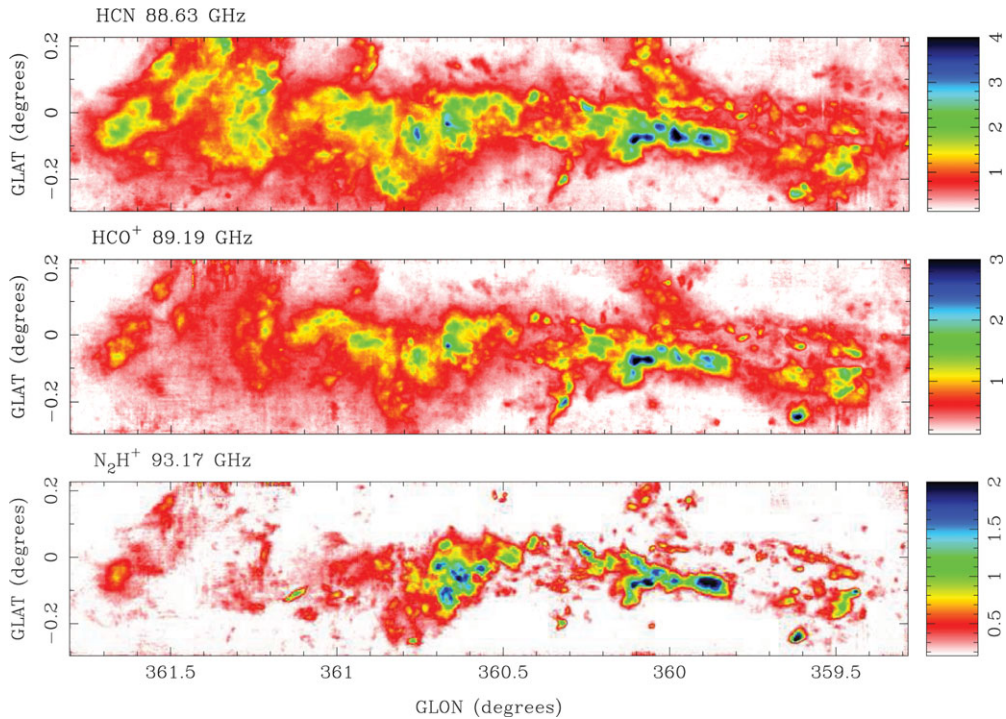
Figure 1. Peak brightness images (T_A^* (K)) for the lines of J=1–0 HCN, HCO$^+$ and N$_2$H$^+$.

Figure 2. The velocity (in km/s) at the emission peak for the N$_2$H$^+$ line. The twisted, rotating dust ring reported by Molinari *et al.* (2011) can be discerned between $l \sim 359.5° - 0.7°$.

observations may be compared we calculated physical parameters for the CMZ in a number of apertures, as shown in Fig. 3. These cover the entire CMZ, as well as the 4 principal dust "cores" (Sgr A, Sgr B2, Sgr C and G1.3).

Table 1 presents the masses of the three most abundant dense core molecules: HCN, HCO$^+$ and HNC. Roughly 50 M$_\odot$ of these molecules exist within the CMZ, 60% being in HCN. This is $\sim 10^{-6}$ the mass of the H$_2$. The four principal cores account for 44% of the dense gas, with the remainder being distributed across the CMZ. However, relatively more HCO$^+$ is found in the dense gas outside the cores than within them (by one-third), whereas the fraction of HNC present in the dense gas varies by a factor of 3 between the cores. Note that ratio w.r.t. CO for these lines varies little (see Table 2), however.
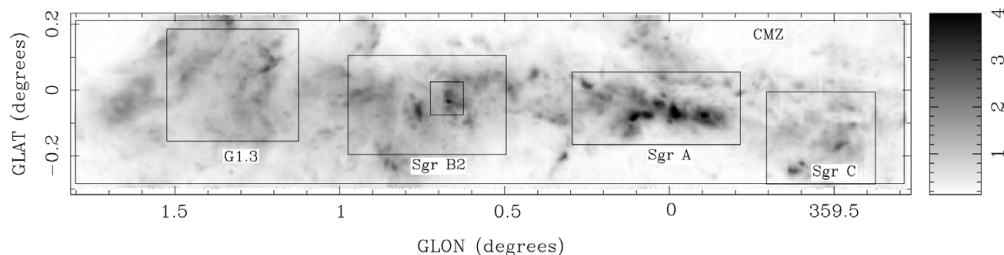
Figure 3. Apertures used for the line luminosity and ratio calculations, overlaid on HCN peak image.

Table 1. Molecular Masses (in $M_\odot$) in the CMZ

Region	HCN	HCO$^+$	HNC	Fraction
CMZ	29	9	11	100%
Sgr A	4	0.8	0.6	10%
Sgr B2	5	1	2	16%
Sgr C	2	0.4	1.5	8%
G1.3	3	0.7	1	9%
Distributed	16	6	6	56%

Masses calculated from the J=1–0 line for each molecule assuming $T_{ex} = 24\,K$, together with an optical depth correction determined from the corresponding ^{13}C isotopologue. The final column shows the fraction of these three molecules in each core relative to the CMZ. 'Distributed' refers to gas outside the 4 cores.

Table 2. Line Luminosities and Line Ratios across the CMZ

Region	CO J=1–0	HCN J=1–0	HCO$^+$ J=1–0	HNC J=1–0	CH$_3$CN J=5–4	HNCO J=4–3	HC$_3$N J=10–9	N$_2$H$^+$ J=1–0	SiO J=2–1
CMZ	2230	212	128	64	11	32	16	32	17
	1.0	1 (-1)	6 (-2)	3 (-2)	5 (-3)	1 (-2)	7 (-3)	1 (-2)	8 (-3)
Sgr A	268	31	19	11	1.7	2.3	2.1	5.7	2.1
	1.0	1 (-1)	7 (-2)	4 (-2)	6 (-3)	9 (-3)	8 (-3)	2 (-2)	8 (-3)
Sgr B2	335	41	25	13	3.1	11	5.2	9.3	4.8
	1.0	1 (-1)	7 (-2)	4 (-2)	9 (-3)	3 (-2)	2 (-2)	3 (-2)	1 (-2)
Sgr C	195	18	11	6.4	0.9	1.0	1.1	2.4	0.6
	1.0	9 (-2)	6 (-2)	3 (-2)	5 (-3)	5 (-3)	6 (-3)	1 (-2)	1 (-2)
G1.3	343	36	20	8.0	1.2	5.3	2.2	4.5	4.7
	1.0	1 (-1)	6 (-2)	2 (-2)	3 (-3)	2 (-2)	6 (-3)	1 (-2)	1 (-2)
Distributed	1090	86	53	26	4	12	5	10	5
	1.0	8 (-2)	5 (-2)	2 (-2)	4 (-3)	1 (-2)	5 (-3)	9 (-3)	4 (-3)

For each region the first row is the line luminosity in units of $10^4\,\mathrm{K\,km\,s^{-1}\,pc^2}$ and the second row the ratio wrt the CO J=1–0 line (from Dame *et al.* 2001).

Line luminosities were also calculated, and compared to CO, as listed in Table 2. In external galaxies often only the CO, HCN, HCO$^+$ and HNC lines are detectable. Their relative fluxes are found to be roughly constant across the CMZ (though we note that the H^{13}CN isotopologue is roughly twice as bright, in comparison to H^{13}CO$^+$, as it is for the corresponding ^{12}C line ratios). HCN/CO ratios across the CMZ are typical of those found in starbursts, albeit at the low end of the observed range.

[$^{12}C/^{13}C$] isotopologue ratios, measured as a function of velocity, generally rise away from the line centre as the main line becomes less optically thick. However, in a few
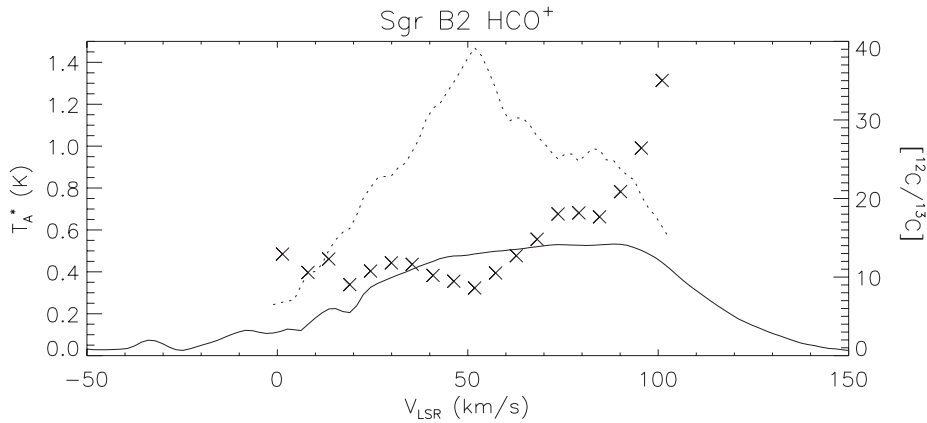
Figure 4. Profile of the HCO^+ line for the Sgr B2 aperture (solid line), and corrected for optical depth (dashed line) assuming a $[^{12}C/^{13}C]$ isotope ratio of 24. The crosses (X) show the $[HCO^+]/[H^{13}CO^+]$ line ratio as a function of velocity. For high positive velocities ($\gtrsim 100\,\mathrm{km\,s^{-1}}$) the ratio is seen to exceed 24.

locations this ratio rises to exceed 24, the isotope ratio considered representative of our galactic nucleus (Langer & Penzias 1990). One such example is shown in Fig. 4 for Sgr B2. At velocities $\gtrsim +100\,\mathrm{km\,s^{-1}}$ the ratio rises to ~ 40, typical of values in the galactic disk. A similar result has also been obtained by Riquelme *et al.* (2010). The $[^{12}C/^{13}C]$ isotope ratio is sensitive to the degree of nuclear processing the gas has experienced, and we speculate that the high values arise due to the infall of less nuclear processed material (i.e. resulting from recent massive star formation) from the disk into the galactic centre along the x_1 and x_2 orbits in the Galaxy's bar potential.

Acknowledgements

References

Dame, T. M., Hartmann, D., & Thaddeus, P. 2001, *ApJ*, 547, 792
Jones, P. A., Burton, M. G., Cunningham, M. R., *et al.* 2008, *MNRAS*, 386, 117
Jones, P. A., Burton, M. G., Tothill, N. F. H., & Cunningham, M. R. 2011, *MNRAS*, 411, 2293
Jones, P. A., Burton, M. G., Cunningham, M. R., *et al.* 2012, *MNRAS*, 419, 2961
Langer W. D. & Penzias A. A. 1990, *ApJ*, 357, 477
Molinari S., *et al.* 2011, *ApJ*, 735, L33
Riquelme D., Amo-Baladrón M. A., Martín-Pintado J., Mauersberger R., Martín S., & Bronfman L. 2010, *A&A*, 523, A51
Walsh, A. J., Breen, S. L., Britton, T., *et al.* 2011, *MNRAS*, 416, 1764